Detection and Classification of {GNSS} Jammers Using Convolutional Neural Networks

Detection and Classification of GNSS Jammers Using Convolutional Neural Networks

Iman Ebrahimi Mehr
Dept. of Electronics and Telecommunications
Politecnico di Torino
Turin, Italy
Iman.ebrahimi@polito.it

Fabio Dovis
Dept. of Electronics and Telecommunications
Politecnico di Torino
Turin, Italy
fabio.dovis@polito.it

***Abstract*—Global Navigation Satellite Systems (GNSSs) have been established as one of the most significant infrastructures in today's world and play an important role in many critical applications. It is known that the power of the GNSS signals at the receivers' antenna is extremely weak and the transmitted signals are vulnerable to interference, which can cause degraded positioning and timing accuracy or even a complete lack of position availability. Thus, it is essential for GNSS applications to detect interference and further recognize the types of it for the mitigation in GNSS receivers to guarantee reliable solutions. In this paper, the focus is on the automatic detection and classification of chirp signals, known as one of the most common and disruptive interfering signals. The classifier is a Convolutional Neural Networks (CNN) based on multi-layer neural networks that operate on the representation of the signals in transformed domains, Wigner-Ville and Short Time Fourier transforms. The representation of signals is fed to a CNN algorithm to classify the different shapes of chirp signals. The proposed method is performed in two case-study scenarios: the monitoring and classification by a terrestrial interference monitor and from a Low-Earth-Orbit (LEO) satellite. The experimental results demonstrate that the CNN model has a classification accuracy of 93% and can be a suitable approach to classify different shapes of chirp signals.**

***Index Terms*—GNSS, Interference, Machine Learning, CNN**

I. Introduction

The widespread use of positioning and timing services based on Global Navigation Satellite Systems (GNSS) includes several applications for which the availability and continuity of such services are of paramount importance. In the presence of Radio Frequency Interference (RFI) on the GNSS bandwidths, the estimation of position and time performed by a GNSS receiver is degraded and, in some cases even totally denied, thus threatening the applications relying on it. RFI can increase the error of the code and phase measurements, consequently, the quality of the constructed pseudoranges [1]. The jamming is usually a simple interference signal of a proper level which is used to intentionally transmit signals with a carrier frequency varying over GNSS bands in a specific area [2]. The existence of jamming signals affects both acquisition and tracking stages in the receiver, which leads to the loss of quality of the GNSS satellite signals [3]. Therefore, The GNSS applications need to detect interference and further recognize the types of interference to mitigate in order to acquire high reliability and prevent a complete lack of positioning.

Various techniques have been proposed to detect RFI at different stages of receivers such as, Automatic Gain Control (AGC) monitoring [4] and Time-domain statistical analysis at Front-end stage [5], Spectral Monitoring and Carrier to Noise power density ratio (C/N_0) Monitoring at the Post-Correlation stage [6]. A successful detection of the threat is rather easy to be obtained since the ultimate goal of jammers is the service denial. However, in presence of jammers if an effective countermeasure has to be applied, it is necessary to estimate the jammer's features in terms of time and frequency behaviour, and not only in terms of an on-off presence. This is a typical *classification* task, that, thanks to the increased computational capabilities of the receiver, can be performed by means of Machine Learning (ML) techniques. The objective of ML algorithm is to automatically extract the most appropriate set of features to build a model that could achieve the desired goal in classification of the jamming signal with high precision [7].

Recently, many works have addressed using ML to detect and classify RFI, working on the time series of digital samples obtained at the output of the receiver front-end. For GPS interference signals [8], the authors implemented the fast independent component analysis method to extract the interference characteristic factors in the frequency domain, time domain, and time-frequency domain and they performed a new algorithm based on a Support Vector Machine (SVM). Similarly in [9], a methodology to classify jammer types was proposed by using two different ML algorithms: SVM and CNN on the set of generated images of time-frequency analysis. According to the conclusion in the classification of the interference and interference-free scenario, it is stated that with a small set of images and not excessively complex parameters, a high accuracy result is obtained. In addition, [10] presents some applications in GNSS that use ML to provide the new solution or new services, and it also showed among the all ML methods, using Neural Network methods offer the best results.

This paper proposes a method for automatic and accurate

978-1-6654-0575-1/22/$31.00

detection of chirp signals based on Convolutional Neural Networks (CNN). The idea is to create an image dataset of images of the signals and feed it into CNN as input in order to detect and classify different types of interference. The effectiveness of the proposed method is demonstrated in two case-study scenarios: the monitoring and classification by a terrestrial interference monitor, and from a Low-Earth-Orbit (LEO) satellite.

II. Methodology

Intentional interference by jammers disrupts GNSS service in a given area of operations and may make the GNSS receivers inoperable. Chirp signals behave differently in terms of time and frequency characteristics, and appropriate analysis of time-frequency domains allow to detect and classify different types of disturbing signals. The time-frequency distributions of a signal can be represented using a variety of approaches such as spectrogram, Wigner-Ville Transform (WVT), or Wavelet transform. In this paper, the spectrogram and WVT have been used to analyze the signal, and since the representation of signals in the time-frequency domain using these two transforms can be stored as images, the proposed method to classify different shapes of chirp signals is image classification.

There are many techniques to perform image classifications. Some of the most common methods are studied to find the best-matched technique according to the desired target, such as CNN, Transfer Learning and SVM. A CNN-based method is considered to achieve a more accurate result in image classification by referring to a study on different introduced techniques [11] [12]. A CNN is a multilayer neural network proposed to identify visual patterns from images represented by pixels with the least pre-processing [13]. The main advantages of using CNN are that pre-trained weights can be shared among different methods, the simplification of computation without losing important data. Finally, it is important to mention that it does not require feature extraction manually, and it's done by the convolution and pooling layers [12].

A general scheme of the methodology is depicted in Figure 1, where the input signals are downconverted to the Intermediate Frequency (IF) and further digitized. Then the transformation is applied to IF digital samples and the representation as an image is used to create image dataset. In the final step, a CNN classifier is implemented for the classification of chirp signals.

A. Short-Time Fourier Transform

Since the frequency of chirp signals change over time, it needs techniques to translates the time-amplitude representation of a signal to a time-frequency representation. Short Time Fourier Transform (STFT) comes to overcome the poor time resolution of the Fourier transform. According to STFT, considering some portion of the non-stationary signal as

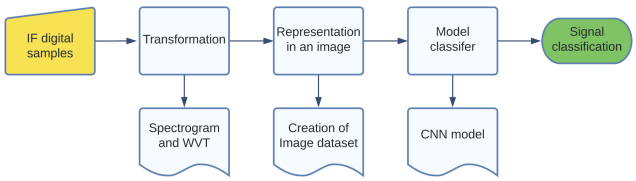

Fig. 1. Diagram explaining the methodology of the research

stationary makes it possible to take the window function of fixed length and move it along the signal [14]. Comparing to Fourier transform in terms of mathematics, formulation looks as follow:

$$F(\omega) = \int_{-\infty}^{\infty} f(t) e^{-i\omega t} dt \tag{1a}$$

$$F(\tau, \omega) = \int_{-\infty}^{\infty} f(t) w(t-\tau) e^{-i\omega t} dt \tag{1b}$$

where τ is translation parameter and $w(t-\tau)$ represents the window function. The only difference with respect to Fourier Transform is the window function where the signal is smoothed. The spectrogram is a representation of the signal's power spectral density which is derived from the squared magnitude of the STFT [15].

B. Wigner-Ville Transform

Basically, there are two approaches to time-frequency analyses, Linear approaches and Quadratic methods. Linear approaches include the Wavelet, Gabor and Zak transform, whereas Quadratic methods cover time-frequency distributions such as the Wigner distribution, smoothed versions of the Wigner distribution and the ambiguity function. Wigner-Ville Transform (WVT) is a time-frequency representation of the signal and a helpful tool to analyze non-stationary signals. The basic idea of this method is to develop a joint function of time and frequency [16].

From theoretical and application points of view, the Wigner-Ville Distribution (WVD) plays a major role in the time-frequency signal analysis for the following reasons. First, it provides a high-resolution representation in both time and frequency for non-stationary signals. Second, it has the special properties of satisfying the time and frequency marginals in terms of the instantaneous power in time, energy spectrum in frequency, and total energy of the signal in the time and frequency plane [17].

WVT essentially computes the Fourier transform of the so-called Auto-correlation FAAunction (AF) $[AF(\tau) = x(t + \tau/2)x^*(t - \tau/2)]$ which is a general representation of the signal's autocorrelation function. The WVT does not suffer from leakage effects as the STFT does and hence, gives the best spectral resolution [18]. There are several presentations in literature for the Discrete Wigner-Ville Transform (DWVT),

the general form ($WV_x[n,m]$) can be written as equation 2 [19] for a signal $x[t]$ where it is sampled by N number.

$$WV_x[n,m] = \sum_{k=-N}^{N} x\left[n+\frac{k}{2}\right] x^*\left[n-\frac{k}{2}\right] e^{-2\pi ikm/N} \quad (2)$$

where x^* denotes the conjugate of x, n and m denote the index numbers for the time and frequency vectors, respectively.

In order to avoid the cross-terms effect in quadratic form, smoothed pseudo Wigner distribution [20] is used to analyse the signal which uses independent windows to smooth in time and frequency and its formulation is as follow:

$$WV_x[n,m] = \sum_{k=-N}^{N} g(n)h(m)x\left[n+\frac{k}{2}\right] x^*\left[n-\frac{k}{2}\right] e^{-2\pi ikm/I} \quad (3)$$

where $h(m)$ represents the lag window function, and $g(n)$ represents the time smooth window function. The length of the signal is used to choose the lengths of Kaiser windows that are used for smoothing in time and frequency.

C. Common jamming signals

The chirp signals are known as one of the most common disruptive or interfering signals with the power to disassemble or block a specific portion of the GNSS signal band and disrupt receiver operations. Chirp is a signal in which its frequency varies with respect to the time; thus, the frequency increment or decrement is known as Up-chirp or Low-chirp, respectively. This type of signal is known as the swept frequency signal. The swept-frequency jammers are distinguished by their ability to generate overwhelming signals with carrier frequencies that vary over GNSS signal bands [21]. According to the survey in [22], chirp signal characteristics can classify in terms of shape, sweep range, sweep rate, and power. Figure 2 shows different types of chirp signals.

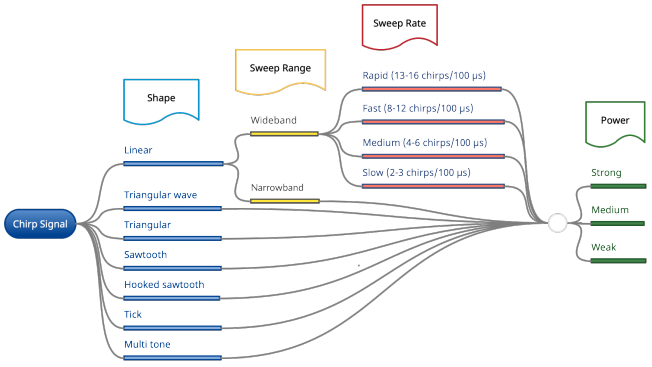

Fig. 2. Chirp Signal Classifications

Table I shows the bandwidth of each chirp signal used in this research, and Figure 3 illustrates the spectrogram of 11 common chirp types and hence most likely that the receiver will encounter.

TABLE I
BANDWIDTH OF CHIRP SIGNALS

Chirp Name	Bandwidth
Wide sweep	16 MHz
narrow sweep	5 MHz
Triangular wave	14 MHz
Triangular	16 MHz
Sawtooth	12 MHz
Hooked sawtooth	14 MHz
Tick	16 MHz
Multi tone	3 MHz

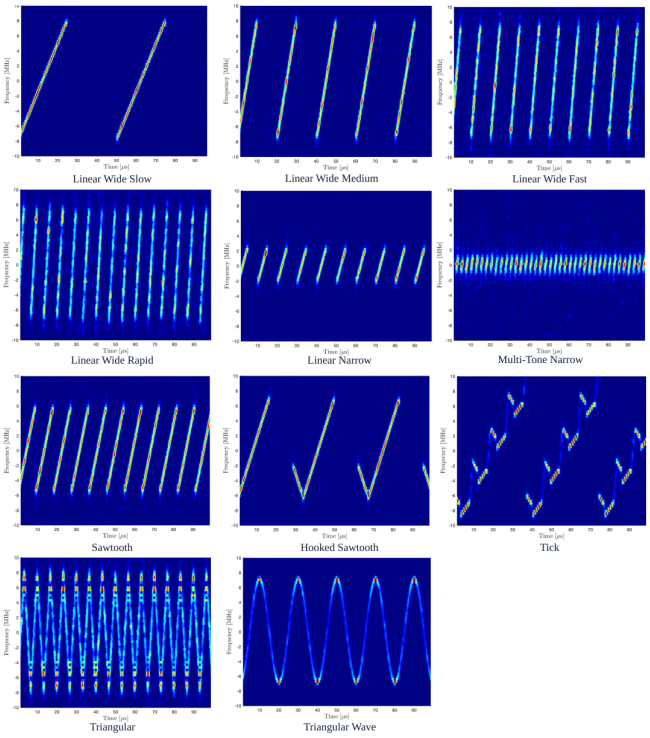

Fig. 3. Spectrogram of 11 common chirp types

D. Convolutional Neural Networks

A Neural Network (NN) is a network of artificial neurons that reflect the way the human brain operates, and many neurons shape a real NN in different layers. NN is made up of several nodes distributed in various layers, and each node implements an instruction called algorithms that guides the machine in identifying patterns in the dataset and solving common problems [23]. What has made NN so famous and influential is CNN: the name comes from after the convolutional operator from the filtering domain. With a linear and timing-variant filter, CNN can filter the input vector extracted from signals, images, and other possible types of data. The CNN becomes powerful in solving different problems by implementing three important concepts [24] as follows:

- Local Receptive Fields: This concept explains using of a new design in such a way that each neuron in the next layer is connected to a subset of the outputs of the

previous layer, instead of using a fully connected neural network. It is rather evident that the number of parameters are extremely decreased.
- Shared weights/biases: this concept implies that all weights and biases in each window of neurons are the same, and consequently, the number of parameters is reduced.
- Pooling Layers: A pooling layer is essentially a down-sampling layer and reduces the data dimensions by combining the outputs of neuron clusters at one layer into a single neuron in the next layer.

III. Result

There are many models of CNN to perform the image classification including, AlexNet [25], GoogleNet [26], SqueezeNet [27]. The performance of these 3 networks is evaluated in terms of the speed of training samples and the accuracy of the classification model. The evaluation of these 3 classifier for the same image dataset (detection of interference on the ground) represent that although the accuracy is almost the same for all three of them, AlexNet is faster compared to the other introduced pre-trained architectures regarding the speed of the training process. The reason is that AlexNet has eight layers of depth with respect to SqueezNet and GoogleNet, which have 18 and 22 layers of depth, respectively.

Alex Krizhevsky primarily designed AlexNet CNN. The input to AlexNet can be a RGB image of size 227×227 pixel that implies all images in the train and test set need to be of size 227×227 pixel. All the images used in this experience are resized to the desired size. In addition, by using a filter, all the input images are changed to grayscale mode. AlexNet comprises 5 convolutional layers and 3 fully connected layers, 3 max-pooling layers, 2 normalization layers, and 1 softmax layer. AlexNet has in total about 60 million parameters and the best initial hyperparameters and configurations derived by a grid search is described in table II.

TABLE II
Initial Hyperparameters and Configuration of AlexNet

Parameter	Value
Minimization Algorithm	Stochastic Gradient Descent Momentum
Initial Learning Rate (λ)	0.001
Batch size	64
Input Image Size	227 x 227
Weight Learn Rate Factor	20
Bias Learn Rate Factor	20
Maximum Number of Epoch	5

The image datasets obtained by transformation are divided into three parts, 70% is used to train the model of CNN, 10% of data is utilized for tuning the parameters of the model (validation dataset) while 20% is dedicated to the evaluation of the model (test dataset). The CNN is trained during five epochs using the Stochastic Gradient Descent Momentum (SGDM) algorithm, which means the all images in the training dataset is passed through the neural network five times both in forward and back-propagation to find the optimal values of the network's parameters. The last step is to assess the trained network, and the evaluation phase provides a performance metric of the trained model on unobserved data. For the evaluation phase of the model, test data is utilized in order to create the confusion matrix. The confusion matrix determines the accuracy of a classification model in the way of how well it predicts the correct and incorrect class for the test data.

The proposed methodology is performed for two different scenarios, detection and classification of interference on the ground and from the space. Each of them is analyzed and simulated using Matlab, and their results are explained as follows.

A. Detection and Classification Interference from the Space

Recent works started to address the idea to monitor the presence of GNSS interference from space [28]. The objective of the GINKO-S project [29] is to perform continuous monitoring of the interference in GNSS navigation bands in low earth orbit on a regional/global scale. The architecture of this monitoring system is basically composed of a NADIR antenna, a Radio Front-End (RFE), and a software processing unit. The NADIR antenna is pointed toward the earth's surface in order to grab possible interference generated on the ground. The RFE is in charge of converting the signal from analog to digital; it first amplifies and filters the analog signal; then, it downconverts the Radio Frequency (RF) signal to an intermediate frequency in order to allow digital conversion. Due to on-board processing limitations, raw samples of interfering received signals are transferred to the ground station, and the classification algorithms are implemented in the ground processor.

Three possible RFE bandwidths (B_{IF}) of 5, 10, and 20 MHz are evaluated, and the sampling frequency is set to $f_s = 2.2 \cdot B_{IF}$ Msamples/s to provide for some margin against the Nyquist frequency. Moreover, the interference signal is embedded in White Gaussian Noise (WGN), where the thermal noise variance over the GINKO bandwidth B_{IF} has been accounted in the margin as well: $\sigma^2_{IF} = N_0 B_{IF}$ where N_0 is noise power spectral density estimated to be $N_0 = -205$ dBW/Hz. In addition, the power of the interference signal received at the LEO satellite is estimated to be in the range between -144 dBW up to -125 dBW.

As explained, in this scenario 3 different datasets of interference signals are simulated considering the RFE bandwidth $B_F = 5, 10, 20$ MHz. The spectrogram and WVT of all the signals are calculated and the output are stored as images in order to create of image datasets. Therefore in total, 6 image datasets are created and each of them consists of 11,000 images (1000 for each class). The CNN model is implemented for each image dataset and the Table III shows their training and test set accuracies.

TABLE III
ACCURACY OF THE MODEL WITH DIFFERENT DATASETS

Bandwidth	Transform	Training Accuracy	Test Accuracy
5 MHz	STFT	82.82 %	80.18 %
10 MHz	STFT	91.9 %	89.31 %
20 MHz	STFT	95.82 %	95.45 %
5 MHz	WV	81.06 %	83.70 %
10 MHz	WV	90.91 %	88.74 %
20 MHz	WV	92.73 %	92.95 %

Table III shows that high accuracy is acquired when the chosen RFE bandwidth is higher because all the entire bandwidth of the chirp signal enter into the RFE, but on the other hand by increasing bandwidth, the sampling frequency is increased, which leads to taking more the time for calculation of the STFT and WVT. The obtained result for both transforms STFT and WVT have almost the same accuracy, but the calculation time of WVT is about 5 times more than STFT. Figure 4 illustrate the confusion matrix of CNN classifier for the RFE bandwidth of 20MHz using STFT analysis.

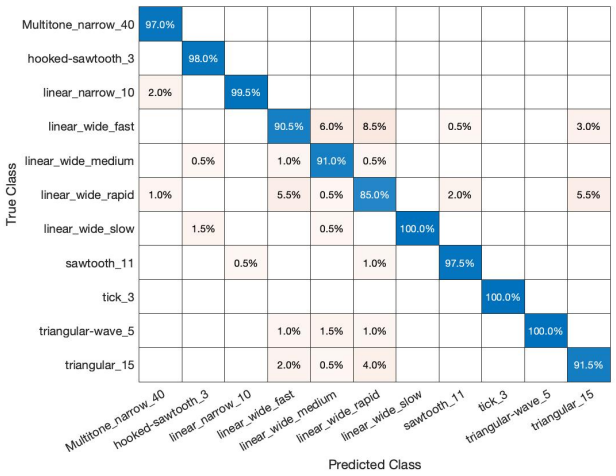

Fig. 4. Confusion Matrix of CNN for bandwidth of 20 MHz

Due to the fact that there are many convolutional layers, including lots of parameters such as weights and biases, the increment of computational time and complexity in the analysis of data is expected. As the next point, the CNN technique has a high accuracy in image classification which is the target of this work.

The main privilege of using CNN over the statistical approach is feature selection done by convolutional layers. Due to the redundant attributes and a large amount of input data in original data sets, feature selection is an important technique for improving neural network performance which uses several convolutional layers to detect the most significant features.

B. Detection and Classification of Interference on the Ground

In this scenario, GNSS signals are simulated using N-FUELS (FULL Educational Library of Signals for Navigation) [30], which is a signal/disturbances generator, implemented as a set of non-real-time Matlab scripts able to simulate the samples of a GNSS signal as seen by the receiver after the Analog to Digital (A/D) conversion. The simulated GNSS signals belong to the GPS constellation and L1 band (1575.42 MHz). Then, totally eight different shapes of chirp signals are generated where their sampling frequency and duration are 40 MHz and $100\mu s$, respectively (the same as the GNSS signal). Despite the different chirp signal shapes, chirp signals' power is amplified from -142 dBW up to -107 dBW, representing medium and strong power. The sweep rate of linear wide-band signal can vary from 2 up to 16 chirp repetitions in 100 microseconds and in the simulation, the case of ten chirp repetitions in 100 microseconds is only considered to have a normal distribution in terms of the number of signals in each class.

Figure 5 illustrates the confusion matrix of the test dataset. It represents that the CNN method for classification has an overall accuracy of 93.46%. The CNN is also able to predict the existence and detect the shape of the chirp signal within the GNSS signal with an accuracy of 92.65%.

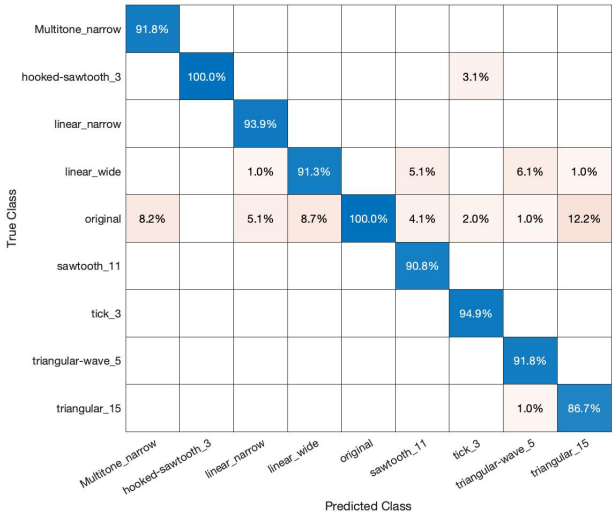

Fig. 5. Confusion Matrix of CNN Algorithm

IV. CONCLUSION

This work performed a full-field analysis method, where CNN classifier is developed in order to identify and classify the chirp interference based on the analysis of the spectrum of the signal. Hence, in this scenario, the datasets included spectrum images. Based on the different studies, the CNN method reportedly has a good performance in image classification problems. This seems to be matched with our

result of applying this algorithm to the dataset.

ACKNOWLEDGMENT

The authors would like to thank the team behind the GINKO project for making this research work possible.

The PhD work of mr Iman Ebrahimi Mehr is supported by the grant DOT1332092 CUP E11B21006430005 funded within the Italian PON "Ricerca e Innovazione" 2014-2020, Asse IV "Istruzione e ricerca per il recupero" con riferimento all'Azione IV.4 "Dottorati e contratti di ricerca su tematiche dell'innovazione" e all'Azione IV.5 "Dottorati su tematiche green". DM 1061/2021.

REFERENCES

[1] D. Borio, F. Dovis, H. Kuusniemi, and L. Lo Presti, "Impact and detection of gnss jammers on consumer grade satellite navigation receivers," *Proceedings of the IEEE*, vol. 104, no. 6, pp. 1233–1245, 2016.

[2] W. Qin, M. T. Gamba, E. Falletti, and F. Dovis, "An assessment of impact of adaptive notch filters for interference removal on the signal processing stages of a gnss receiver," *IEEE Transactions on Aerospace and Electronic Systems*, vol. 56, no. 5, pp. 4067–82, 2020.

[3] M. Tamazin, M. Karaim, H. Elghamrawy, and A. Noureldin, "A comprehensive study of the effects of linear chirp jamming on gnss receivers under high-dynamic scenarios," in *2018 13th International Conference on Computer Engineering and Systems (ICCES)*, 2018, pp. 9–14.

[4] H. Borowski, O. Isoz, F. Eklof, S. lo, and D. Akos, "Detecting false signals: With automatic gain control," *GPS world*, vol. 23, pp. 38–43, 04 2012.

[5] K. Sun, T. Jin, and D. Yang, "An improved time-frequency analysis method in interference detection for gnss receivers," *Sensors (Basel, Switzerland)*, vol. 15, pp. 9404–26, 04 2015.

[6] E. Falletti, M. Pini, and L. L. Presti, "Low complexity carrier-to-noise ratio estimators for gnss digital receivers," *IEEE Transactions on Aerospace and Electronic Systems*, vol. 47, no. 1, pp. 420–437, 2011.

[7] P. Flach, *Machine Learning: The Art and Science of Algorithms That Make Sense of Data*. Cambridge University Press, 01 2012.

[8] J. Xu, S. Ying, and H. Li, "Gps interference signal recognition based on machine learning," *Mobile Networks and Applications*, vol. 25, 12 2020.

[9] R. Ferre, A. Fuente, and E. S. Lohan, "Jammer classification in gnss bands via machine learning algorithms," *Sensors*, vol. 19, p. 4841, 11 2019.

[10] A. Siemuri, H. Kuusniemi, M. S. Elmusrati, P. Välisuo, and A. Shamsuzzoha, "Machine learning utilization in gnss—use cases, challenges and future applications," in *2021 International Conference on Localization and GNSS (ICL-GNSS)*, 2021, pp. 1–6.

[11] T. Maruyama, N. Hayashi, Y. Sato, S. Hyuga, Y. Wakayama, H. Watanabe, A. Ogura, and T. Ogura, "Comparison of medical image classification accuracy among three machine learning methods," *Journal of X-Ray Science and Technology*, vol. 26, pp. 1–9, 09 2018.

[12] K. Sanghvi, A. Aralkar, S. Sanghvi, and I. Saha, "A survey on image classification techniques," *SSRN Electronic Journal*, 01 2021.

[13] K. Sanghvi and et al, "Fauna image classification using convolutional neural network," *International journal of future generation communication and networking*, vol. 13, pp. 8–16, 05 2020.

[14] C. Mateo and J. Talavera, "Short-time fourier transform with the window size fixed in the frequency domain," *Digital Signal Processing*, vol. 77, pp. 13–21, 2018.

[15] E. Klejmova and J. Pomenkova, "Identification of a time-varying curve in spectrogram," *Radioengineering*, vol. 26, no. 1, pp. 291–298, 2017.

[16] B. Boashash and P. Black, "An efficient real-time implementation of the wigner-ville distribution," *IEEE Transactions on Acoustics, Speech, and Signal Processing*, vol. 35, no. 11, pp. 1611–1618, 1987.

[17] L. Debnath and F. A. Shah, "The wigner-ville distribution and time-frequency signal analysis," in *Wavelet Transforms and Their Applications*, 2015, pp. 287–336.

[18] J. O' Toole, M. Mesbah, and B. Boashash, "A discrete time and frequency wigner-ville distribution: properties and implementation," in *International Symposium on Digital Signal Processing and Communication Systems*, 01 2005.

[19] L. Cohen and P. Loughlin, "leid1. time-frequency analysis: Theory and applications," *The Journal of the Acoustical Society of America*, vol. 134, no. 5, pp. 4002–4002, 2013.

[20] L. Stankovic, "A method for time-frequency analysis," *IEEE Transactions on Signal Processing*, vol. 42, no. 1, pp. 225–229, 1994.

[21] W. Qin, M. Troglia Gamba, E. Falletti, and F. Dovis, "Effects of optimized mitigation techniques for swept-frequency jammers on tracking loops," *Proceedings of the 32nd International Technical Meeting of the Satellite Division of The Institute of Navigation (ION GNSS+ 2019)*, pp. 3275–3284, 10 2019.

[22] Strike3 project, d6.2: Threat database analysis report. European GNSS Agency (GSA). [Online]. Available: http://gnss-strike3.eu

[23] A. Geron, *Hands-On Machine Learning with Scikit-Learn, Keras, and TensorFlow, 2nd Edition*. O'Reilly Media, Inc., 2019.

[24] R. Yamashita, M. Nishio, R. Do, and K. Togashi, "Convolutional neural networks: an overview and application in radiology," *Insights into Imaging*, vol. 9, p. 611–629, 06 2018.

[25] A. Krizhevsky, I. Sutskever, and G. E. Hinton, "Imagenet classification with deep convolutional neural networks," *Communications of the ACM*, vol. 60, no. 6, p. 84–90, may 2017.

[26] C. Szegedy, W. Liu, Y. Jia, P. Sermanet, S. Reed, D. Anguelov, D. Erhan, V. Vanhoucke, and A. Rabinovich, "Going deeper with convolutions," *The IEEE Conference on Computer Vision and Pattern Recognition (CVPR)*, pp. 1–9, 06 2015.

[27] F. Iandola, M. Moskewicz, K. Ashraf, S. Han, W. Dally, and K. Keutzer, "Squeezenet: Alexnet-level accuracy with 50x fewer parameters and textless1mb model size," *arXiv preprint arXiv:1602.07360*, 02 2016.

[28] M. J. Murrian, L. Narula, P. A. Iannucci, S. Budzien, B. W. O'Hanlon, M. L. Psiaki, and T. E. Humphreys, "First results from three years of gnss interference monitoring from low earth orbit," *NAVIGATION, Journal of the Institute of Navigation*, vol. 68, no. 4, pp. 673–685, 2021.

[29] Ginko-s (gnss interference monitoring and notification to key operators from space). European Space Agency. [Online]. Available: https://navisp.esa.int/project/details/164/show

[30] E. Falletti, D. Margaria, M. Nicola, G. Povero, and M. Troglia Gamba, "N-fuels and soprano: Educational tools for simulation, analysis and processing of satellite navigation signals," in *2013 IEEE Frontiers in Education Conference (FIE)*, 10 2013, pp. 303–308.